ISSN 2616-5767 Vol.8, Issue 4: 110-120, DOI: 10.25236/AJETS.2025.080415

Parameters Optimization Method of Milling Aerospace Blade Milling Based on Black Hole Continuous Ant Colony Algorithm

Weiluo Wang[1,*], Zi Wang[2]

[1]*College of Mechanical Engineering, Chongqing University of Technology, Chongqing, China, 400054*
[2]*School of Smart City and Transportation, Southwest Jiaotong University, Chengdu, China, 611756*
[*]*Corresponding author: wangqeiluo@stu.cqut.edu.cn*

Abstract: *The existing parameter optimization methods tend to fall into local optimization, and it is difficult to balance the contradiction between machining time and deformation, resulting in low machining efficiency and unstable surface quality. To address the above problems, a multi-objective optimization method combining the black hole algorithm and continuous ant colony algorithm (BH-ACO_R) is proposed. In terms of the algorithm, the black hole mechanism is introduced to, divide the solution file into "black holes" (the first k superior solutions) and "planets" (the last m inferior solutions), the exploration ability of the solution space is improved through the global search of the planets to the black holes and the local perturbation strategy of the black holes. A normalized weighted objective function is defined to balance the time efficiency and the weighting requirements of aerospace blade milling. Finally, the algorithm is simulated using MATLAB, compare with the traditional methods. The BH-ACO_R algorithm reduces the machining time by 17.3%, reduces the amount of deformation by 15.6%, and improves the convergence speed by 22%, which verifies its effectiveness and engineering applicability in complex multi-objective optimization.*

Keywords: *BH-ACO_R, Aerospace Blade, ACO_R*

1. Introduction

The manufacturing sector, particularly in aerospace and automotive industries, is being transformed toward intelligent manufacturing. As a representative of highly complex components with both military and civilian applications, the aero-engine blades play a crucial role in ensuring the stable operation of aircraft engines, where their machining accuracy is of paramount importance. Consequently, data-driven precision machining has emerged as the dominant approach in manufacturing to enhance the surface quality of high-precision components [1-3].

Extensive research efforts have been devoted to enhancing the performance and service life of aviation blades through various experimental approaches. A machining parameter optimization methodology was developed by some scholar based on milling force modeling, where the ploughing effect at the tool tip was effectively mitigated through comprehensive analysis of cutting forces and ball-end mill orientation dynamics during milling operations [4]. While this approach demonstrated significant improvement in surface quality, its applicability was primarily limited to planar milling operations, with insufficient investigation into complex surface machining.

In related work, LAN et al. [5] conducted systematic research on deformation control in aero-engine blade machining. Key deformation factors in blade milling processes were identified and analyzed, leading to quality improvements through advanced process control strategies. However, the practical implementation of this method was constrained to specialized applications with limited operational flexibility.

An alternative approach was proposed by Song et al. [6], featuring double-tool milling of turbine blades with toolpath optimization through equivalent parameter path planning. This technique achieved two-fold efficiency enhancement compared to conventional single-tool machining while improving profile accuracy. Nevertheless, the methodology was principally applicable to large-scale blade processing, exhibiting restricted generalizability. Despite these advancements in multi-objective optimization for aviation blade milling, significant challenges persist. Current optimization algorithms are frequently trapped in local optima, demonstrating limited capability in balancing multiple objectives.

ISSN 2616-5767 Vol.8, Issue 4: 110-120, DOI: 10.25236/AJETS.2025.080415

This limitation stems primarily from empirical dependence in weight allocation between machining time and deformation control, coupled with inadequate adaptive mechanisms. The continuous ant colony algorithm (ACO_R) has shown superior performance in continuous function optimization compared to its discrete counterpart, delivering higher solution accuracy with successful engineering applications [7]. However, while ACO_R exhibits rapid convergence [8], its inherent inferior solution elimination mechanism during iteration often results in premature convergence to local optima without effective escape mechanisms.

To address the aforementioned challenges, a black hole continuous ant colony algorithm ($BH-ACO_R$,) is proposed in this study. In this algorithm, the black hole mechanism is integrated, where the solution archive is divided into two categories: "black hole" representing elite solutions and "planet" denoting inferior solutions. The global search capability is enhanced through gravitational attraction exerted by planets toward black holes, while convergence precision is improved by incorporating local perturbation operations around black holes.

Through the implementation of a dynamic weighting strategy, a normalized weighted objective function is designed, where the processing time and machining deformation requirements are balanced in real-time by an adaptive weight coefficient. Furthermore, a nonlinear regression model is established between milling parameters (n, a_e ,f, a_p) and performance objectives (T, P). This model is constructed based on comprehensive data analysis involving 4-factor 3-level orthogonal experiments and 29 sets of experimental data fitting.

2. Parameters optimization Method for Aero-engine Blade Milling

2.1 Process Parameters

Figure. 1shows that one of the main processes of metal material processing and molding. in the cutting process, the best milling process parameters are optimized to the attention of the manufacturing industry [9]. Optimization of milling process parameters can better improve the machining efficiency and reduce the machining deformation.

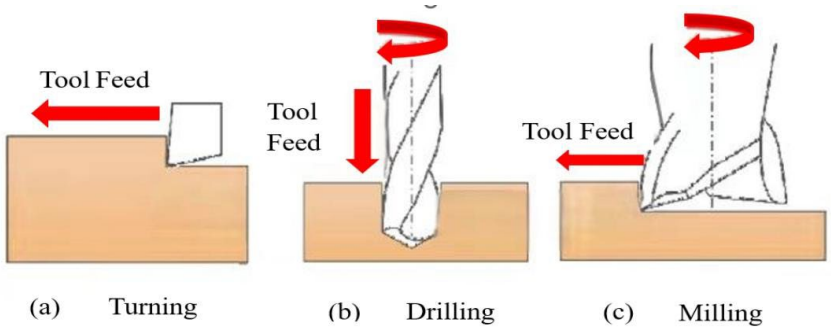

Figure 1 Machining Method

However, during aerospace blade machining (be shown in figure 2), excessive back draft and feed per tooth can degrade blade profile quality, increase surface roughness (Ra), and produce prominent, persistent cutter marks. Conversely, while higher spindle speeds may reduce cutting forces, they can accelerate tool wear and compromise milling efficiency.

Figure 2 Aerospace blade structure

ISSN 2616-5767 Vol.8, Issue 4: 110-120, DOI: 10.25236/AJETS.2025.080415

In this study, four key milling parameters were selected as independent variables: spindle speed (n), milling depth (a_p), feed per tooth (f), milling width (a_e), The machining efficiency was evaluated through machining time (T), while workpiece deformation (P) served as the quality metric.

2.2 Machining tool and material parameters

The mechanical milling process varies significantly depending on precision requirements. Tool selection must account for multiple factors including workpiece material, machining process, precision specifications, and machine tool capabilities. For blade milling operations, ball-end milling cutters are predominantly employed. Table 1 presents the tool's structural parameters, which were determined based on the specific requirements of the blade machining process.

Table 1 Structure parameters of ball end milling cutter

Tool Diameter(mm)	Cutting Radius(mm)
6	0.02
Rake Face Length (mm)	Flank Face Length (mm)
4	4
Rake Angle (°)	Clearance Angle (°)
5	10
Tool Material	Initial Temperature (℃)
Carbide-Grade-K	20

2.3 Analysis of the influence of parameters on the whole milling process

Spindle speed: the rotational speed per minute of the milling tool on the spindle, the increase in spindle speed can lead to increased tool wear, with a decrease in cutting force, which is expressed by (1).

$$n = \frac{1000\mathrm{v}_c}{\pi D_{cap}} \tag{1}$$

Where $\mathrm{v}_c$is the cutting speed, and $D_{cap}$is the cutting diameter at the actual depth.

Milling depth (a_p): Defined as the radial engagement between the tool and workpiece (the difference between final and initial cut radii), milling depth significantly influences cutting mechanics. Increasing a_p typically elevates both cutting forces and temperatures, potentially inducing workpiece deformation. Excessive depths may also compromise surface integrity due to heightened tool-workpiece interactions.

Milling Width (a_e): The radial cutting width during tool engagement. Larger a_e values generally increase cutting forces and, at constant depth and feed conditions, may degrade surface finish (higher Ra values). This effect stems from greater tool deflection and vibration at wider engagements

Feed per tooth (f_z): Feed per tooth (f_z) represents the axial material removal per cutting edge per revolution ($mm/tooth$), determined by the ratio of feed rate to rotational speed. As a key process determinant, feed per tooth directly modulates three fundamental aspects.

(1) Cutting force magnitude/spatial distribution.

(2) Thermal energy accumulation in the shear zone.

(3) Surface integrity - with f_z elevated values particularly compromising blade quality through heightened R_a values and visible feed marks.

$$f_z = \frac{v_f}{\mathrm{n} \times z_c} \tag{2}$$

Where v_f is the table feed speed.

The processing time efficiency can be quantified through the following model:

$$t_w = 1 + \frac{\pi dL}{1000 v f_z} + t_{ct}\frac{\pi dL}{K c_T v^{1+x_t} {f_z}^{1+y_t} {a_e}^{z_t} {a_p}^{w_t}} + t_{0t} \tag{3}$$

Where $K = 1000$, t_w is the machining time, t_{ct} is each tool change time; t_{0t} is other auxiliary time, d is the tool diameter, L is the length of the workpiece machining, Z is the number of teeth of

ISSN 2616-5767 Vol.8, Issue 4: 110-120, DOI: 10.25236/AJETS.2025.080415

the tool, c_T is the total number of parameters affecting the service life of the tool. The weighting coefficients $x_t, y_{t,} z_{t,} w_t$ represent the relative influence of their corresponding parameters on tool life. Through analysis of production data and existing research findings, the feasible ranges for these process parameters were determined and are presented in the experimental design matrix. Experimental data for machining-induced plastic deformation and processing time are presented in Table 2.

Table 2 4-factor 3-level experimental design

Input Parameters	Coded Level		
	-1	0	1
f(mm/r)	0.05	0.175	0.3
n (r/min)	800	1900	3000
ae (mm)	0.1	0.45	0.8
ap (mm)	0.1	0.45	0.8

The model coefficients and exponents were initially derived from standard cutting parameter handbooks. However, when encountering non-standard machining conditions not covered in these references, empirical determination through experimental data fitting becomes necessary. This study adopts published experimental data from prior work [10], with the time efficiency (T) and machining deformation (P) coefficients being determined through nonlinear regression analysis of the referenced dataset (be shown in Table 3)

Table 3 Statistics of blade milling process

NO	f(mm/r)	n(r/min)	ae(mm)	ap(mm)	T(s)	PS
1	-1	-1	0	0	10979	2.02
2	-1	0	-1	0	20618	1.56
3	-1	1	0	0	2928	1.79
4	-1	0	0	-1	4623	1.68
5	-1	0	1	0	2626	1.70
6	-1	0	0	1	4623	1.86
7	0	0	0	0	1320	3.50
8	0	0	-1	-1	5890	3.15
9	0	0	0	0	1320	3.50
10	0	0	0	0	1320	3.54
11	0	0	0	0	1320	3.94
12	0	1	0	1	837	2.70
13	0	-1	1	0	1782	3.50
14	0	1	-1	0	3730	2.67
15	0	1	0	-1	837	2.58
16	0	0	1	1	750	3.78
17	0	1	1	0	475	4.02
18	0	-1	0	-1	3137	3.70
19	0	-1	-1	0	13990	3.29
20	0	-1	0	1	3137	3.83
21	0	0	-1	1	5890	3.26
22	0	0	0	0	1320	3.44
23	0	0	1	-1	750	3.70
24	1	0	1	0	438	3.06
25	1	1	0	0	488	2.83
26	1	0	-1	0	3437	3.09
27	1	0	0	-1	770	2.72
28	1	-1	0	0	1830	3.43
29	1	0	0	1	770	2.54

Through analysis of variance ($ANOVA$) performed on 29 validated datasets of machining time and deformation, we derived empirical regression models for machining time (T) and machining deformation (P), by (4) and (5).

$$T = 35227.68 - 1.112 \times 10^5 f - 4.553n - 58281.1045a_e + 7.4739 \times 10^{-13} a_p$$
$$+85674.2857 f a_e + 5.8136 n a_e + 1.3394 \times 10^5 f^2 + 23460.1113 {a_e}^2 \quad (4)$$

ISSN 2616-5767 Vol.8, Issue 4: 110-120, DOI: 10.25236/AJETS.2025.080415

$$P = 0.6188 + 28.5882f - 0.00024n + 0.6603a_e + 0.1031a_p - 68.2163f^2 \quad (5)$$

Based on the mathematical formulations of machining efficiency and workpiece deformation, subject to operational constraints, we establish the multi-objective optimization model for high-efficiency, low-deformation milling of aerospace blades as follows

$$\min T = \min\begin{pmatrix} 35227.68 - 1.112 \times 10^5 f - 4.553n - 58281.1045a_e + 7.4739 \times 10^{-13}a_p \\ +85674.2857fa_e + 5.8136na_e + 1.3394 \times 10^5 f^2 + 23460.1113{a_e}^2 \end{pmatrix} \quad (6)$$

$$minP = \min\left(0.6188 + 28.5882f - 0.00024n + 0.6603a_e + 0.1031a_p - 68.2163f^2\right) \quad (7)$$

$$\begin{cases} 0.05 \le f \le 0.3 \\ 800 \le n \le 3000 \\ 0.1 \le a_e \le 0.8 \\ 0.1 \le a_p \le 0.8 \end{cases} \quad (8)$$

Multi-objective optimization problems are commonly transformed into single-objective formulations through weighted sum approaches. However, given the disparate magnitudes of machining time (T) and machining deformation (P), normalization of both objective functions is required. To accommodate distinct performance priorities, we assign differential weighting coefficients (α, β) such that

(1) A larger α coefficient emphasizes milling time efficiency (minimizing T)

(2) A larger β coefficient prioritizes deformation reduction (minimizing P)

Where $\alpha + \beta = 1$, reflecting the trade-off between these competing objectives

The weighted multi-objective function can be formulated as

$$minF = \min[kt_w^* + (1-k)P^*] \quad (9)$$

The weighting coefficients k and $1-k$ represent the relative importance of milling time efficiency and machining deformation, respectively, where k takes discrete values from 0.1 to 0.9 in increments of 0.1. The normalized objective functions are denoted as t_w^* (for milling time efficiency) and P^* (for machining deformation)

The normalization operation is mathematically expressed as

$$f = \frac{f_i - f_{i,min}}{f_{i,max} - f_{i,min}} \quad (10)$$

Where $f_{i,max}$ and $f_{i,min}$ are the maximum and minimum values for single-objective optimization of each objective function, respectively.

2.4 Traditional optimization methods

The ant colony optimization (ACO) algorithm exhibits strong global search capabilities and robustness to initial conditions, demonstrating the ability to converge to optimal solutions even with non-uniform initial pheromone distributions. However, conventional ACO suffers from slow convergence rates and a tendency to become trapped in local optima. To address these limitations, researchers have developed the continuous ant colony algorithm (ACO_R), which enhances the standard ACO framework through Gaussian kernel sampling for solution generation. This extension enables effective optimization in continuous search spaces, significantly expanding the algorithm's applicability to continuous optimization problems.

Step 1, Archive Initialization

During algorithm initialization, the archive size is set to K (termed as K-archive).

In each iteration, the archive only retains (be shown in figure 3)

(1) Position vectors of the top K fitness-ranked individuals are $n_1 = \{n_l^1, n_l^2, \ldots n_l^m\}$

(2) Corresponding fitness values is $f(s_l)$.

ISSN 2616-5767 Vol.8, Issue 4: 110-120, DOI: 10.25236/AJETS.2025.080415

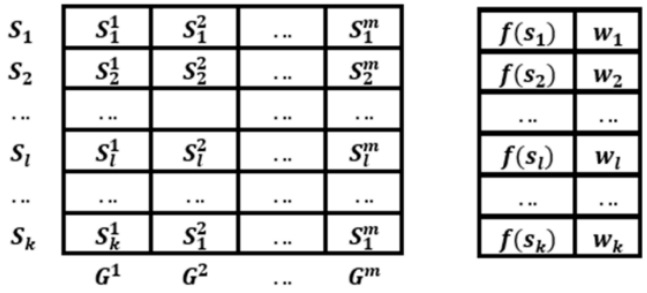

Figure 3 illustrates the internal architecture of the archive

Step 2, Dynamic Weight-based Pheromone Update Strategy

The algorithm employs an adaptive pheromone update mechanism that dynamically adjusts pheromone concentrations based on both current pheromone levels and iterative optimization results. Individuals in the archive are sorted in ascending order of fitness value (where lower fitness values indicate better solutions), such that

$$f(s_1) < f(s_2) \ldots < f(s_l) \ldots < f(s_k)$$

Correspondingly, the weight assignment follows a monotonically decreasing sequence

$$w_1 > w_2 \ldots > w_l \ldots > w_k$$

The weight distribution is calculated as follows

$$w_l = \frac{1}{\mathrm{q}k\sqrt{2\pi}} e^{\frac{(1-l)^2}{2q^2k^2}} \tag{11}$$

Where q is a reinforcement factor, the smaller its value the more the algorithm tends to hang on to the pre-ordered solution.

Step 3, Solution Selection Probability Calculation

The selection probability P_i for each solution is computed as follows

$$P_i = \frac{w_i}{\sum_{i=0}^{n} w_i} \tag{12}$$

Step 4, Guided Solution Sampling

Using the selection probabilities P_i obtained in Step 3, a guide solution x_i is chosen to generate m samples across n dimensions. This sampling process employs a weighted Gaussian kernel function $G_i(x)$, defined as

$$G_i(x) = \sum_{i=0}^{n} w_i \, g_{ij}(x) = \sum_{i=0}^{n} w_i \frac{1}{\sigma_{ij}\sqrt{2\pi}} e^{\frac{(1-l)^2}{2q^2k^2}} \tag{13}$$

Where $j = 1,2, \ldots, n; \mu_{ij}$ is the mean , $\mu_{ij} = x_{ij}$, σ_{ij} is the standard deviation.

$$\sigma_{ij} = \xi \sum_{e=0}^{k} \frac{|x_{ej} - x_{ij}|}{k-1} \tag{14}$$

Where ξ is the offset distance ratio, whose value is greater than 0. The larger the ξ value, the slower the algorithm converges.

Final Step, Solution Archive Update

Following the sampling process, the algorithm

(1) Generates m new candidate solutions (ants)

(2) Computes their objective function value $F(x_i)$ using the weighted evaluation formula

(3) Combines them with the existing k solutions in the archive

ISSN 2616-5767 Vol.8, Issue 4: 110-120, DOI: 10.25236/AJETS.2025.080415

(4) Sorts the combined $(k+m)$ solutions in ascending order of $F(x_i)$ values

(5) The archive is updated by retaining the top k solutions while discarding the bottom m solutions.

The archive updating process iterates until the termination criteria are met.

3. Black hole continuous ant colony algorithm ($BH-ACO_R$)

Algorithm structure: The algorithm is characterized by its dual-processing approach for both superior and inferior solutions in the solution archive during the final phase of ACO_R. The top k high-quality solutions are designated as black holes (elite solutions), while the remaining m inferior solutions are treated as planets (suboptimal solutions). Each planet is gravitationally attracted toward all black holes to facilitate global exploration, whereas black holes maintain mutual non-attraction to preserve solution quality - this dynamic interaction enhances search space coverage and solution diversity. Concurrently, an intensive local search strategy is applied to each black hole to refine optimization precision. For the specific case of optimizing four cutting parameters (n =4), the architectural configuration of the resulting four-dimensional solution archive is illustrated in Figure 4.

	n	f	a_p	a_e	
x_1	x_1^1	x_1^2	x_1^3	x_1^4	$F(x_1)$
x_2	x_2^1	x_2^2	x_2^3	x_2^4	$F(x_2)$
⋮	⋮	⋮	⋮	⋮	⋮
x_k	x_k^1	x_k^2	x_k^3	x_k^4	$F(x_k)$
x_{k+1}	x_{k+1}^1	x_{k+1}^2	x_{k+1}^3	x_{k+1}^4	$F(x_{k+1})$
⋮					
x_{k+m}	x_{k+m}^1	x_{k+m}^2	x_{k+m}^3	x_{k+m}^4	$F(x_{k+m})$

Figure 4 Structure of the four-dimensional solution file

Within the search space constrained by the multi-objective function, when randomly initializing k ants, the position vector of the i-th ant (comprising 4 decision variables) can be mathematically represented as

$$x_i = (x_i^1, x_i^2, x_i^3, x_i^4) = (n_i, f_i, a_{pi}, a_{ei}) \tag{15}$$

During the iterative process encompassing Steps 2-4 of ACO_R the algorithm generates m new candidate solutions. Given the four-dimensional parameter space of milling optimization, excessive sampling ($m \gg 50$) would induce solution redundancy due to the limited parametric combinations, consequently impairing optimization efficiency. Therefore, this study empirically sets m = 50 through preliminary experimentation. Following the weighted objective function evaluation and solution ranking, the archive update mechanism operates as follows: (1) the top k solutions exhibiting superior trade-offs between machining time and workpiece deformation are designated as elite solutions (black holes); (2) the remaining m solutions are classified as exploratory solutions (planets) for subsequent global search operations.

The global search mechanism governs the motion of planetary solutions toward the elite set (black holes), generating m new solution vectors according to the following stochastic search operator.

$$X_{i,j} = X_{i,j} + \left(X_{b,j} - X_{i,j}\right) \cdot rand(0,1) \tag{16}$$

Where i is the ith planet, $i = 1,2,\ldots,50$, b is the bth black hole, $b = 1,2,\ldots,k$, j is the jth dimension, j=1,2,3,4, j is the position of the ith planet in the jth dimension, $X_{b,j}$ is the position of the bth black hole in the jth dimension.

Since a black hole can absorb matter around it, when a planet completes its movement, if it enters within the absorption radius R_b of the black hole, it will be absorbed by the black hole. To ensure the total number of planets in the search space remains constant, an equivalent number of planets must be replenished in the search space for those absorbed by the black hole, with the condition that the newly generated planets are not within the absorption radius R_b. For multi-objective optimization problems, the calculation of the absorption radius R_b is defined as

$$R_b = \left| \frac{F_b}{\sum_{i=1}^{m} F_i} \right| \tag{17}$$

ISSN 2616-5767 Vol.8, Issue 4: 110-120, DOI: 10.25236/AJETS.2025.080415

Where F_b is the magnitude as a function of the b black hole, and F_i is the magnitude as a function of the first i planet.

For black holes, the primitive black hole algorithm considers that it has a better function value than planets and does not allow the black hole to generate movement. However, for the optimization problem of milling parameters for aerospace blades, it is possible to have a globally optimal solution near the black hole. In order to improve the accuracy of the solution, the $BHG-ACO_R$ algorithm makes k black holes search locally in the space of radius R_b and then generates new k solutions. The process of localized search of black holes can be expressed as

$$X_{i,j} = X_{b,j} + rand \cdot R_b \tag{18}$$

Finally, the $2m+2k$ solutions related to planets and black holes are sorted and the top k solutions are taken to update the solution archive before entering a new round of iterative computation.

4. Analysis of Optimization Results

To address the bi-objective optimization problem minimizing both machining time (T) and workpiece deformation (P) in aerospace blade milling, A MATLAB implementation of the $BH-ACO_R$ hybrid algorithm is developed. The computational framework incorporates (be shown in figure 5).

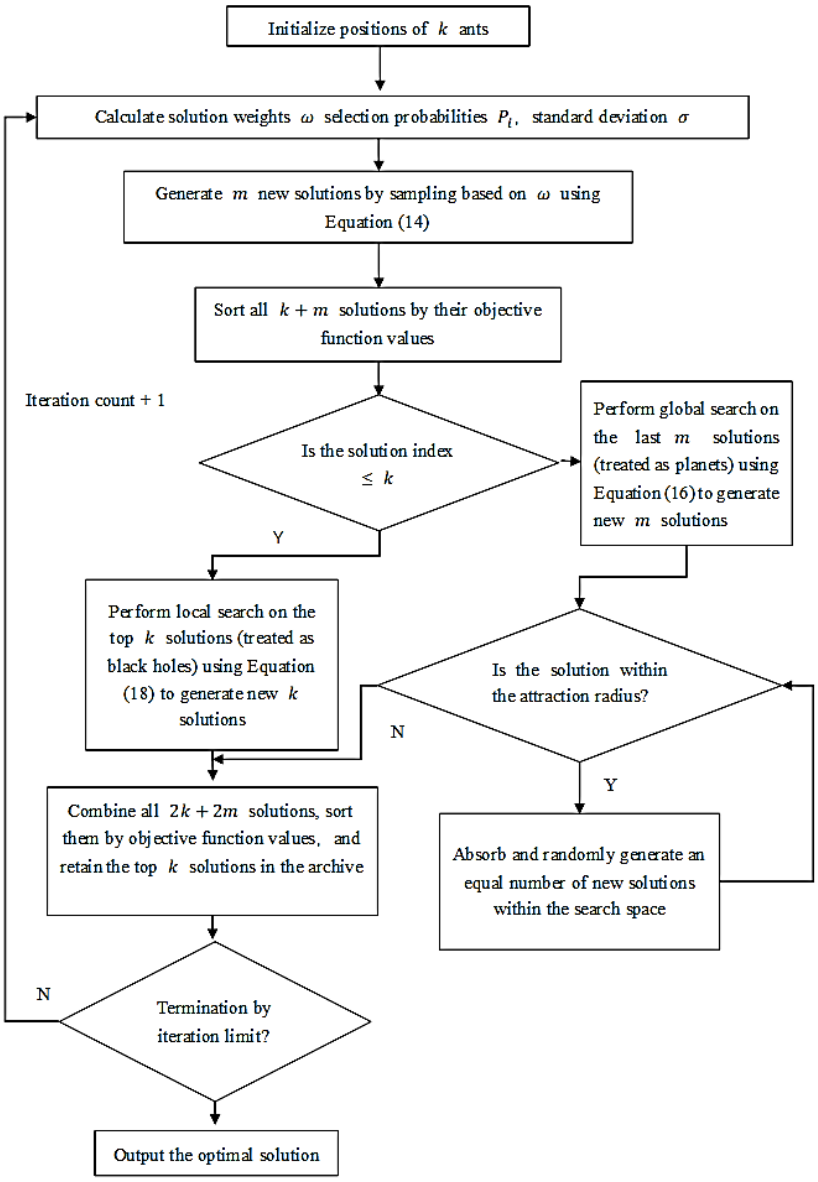

Figure 5 $BH-ACO_R$ flow chart

ISSN 2616-5767 Vol.8, Issue 4: 110-120, DOI: 10.25236/AJETS.2025.080415

The parameter settings of $BH-ACO_R$ are presented in Table 4.

Table 4 $BHG-ACO_R$ parameter settings

Parameter	Value
Number of Iterations	200
Initial Population Size k	10
Reinforcement Factor q	0.5
Offest Distance Ratio	0.8

When the weight coefficient c of the multi-objective optimization function is set to 0.5, the search results of the cutting parameters at the 50th, 100th, and 200th generations, the search results have converged, with the position of the black concentrated hole at v_c= 811.36 m /min, feed per tooth f= 0. 05 mm /r, milling width a_e= 0. 1 mm, and milling depth a_p=0.1mm, indicating the presence of optimal cutting parameter values.

The optimization results of specific cutting energy and surface roughness corresponding to different weight coefficient c values are presented in Table 5.

Table 5 Optimization results under different weights

c	v_c	a_p	f	a_e	t	P
0.1	877.51300429	0.1	0.05	0.1	0.89301300	0.09400130
0.2	838.93609206	0.1	0.05	0.1	0.85443609	0.09014361
0.3	809.14604836	0.1	0.05	0.1	0.82464605	0.08716460
0.4	885.11659911	0.1	0.05	0.1	0.90061660	0.09476166
0.5	811.36846893	0.1	0.05	0.1	0.82686847	0.08738685
0.6	817.97995317	0.1	0.05	0.1	0.83347995	0.08804800
0.7	804.98730209	0.1	0.05	0.1	0.82048730	0.08674873
0.8	899.94138648	0.1	0.05	0.1	0.91544139	0.09624414
0.9	906.65383783	0.1	0.05	0.1	0.92215384	0.09691538

From Table 5, it can be seen that the optimized optimal cutting speed is close to 811.3 m/min.

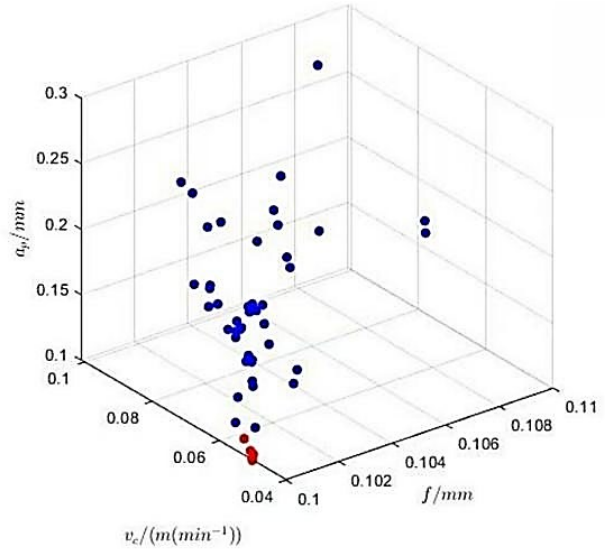

Figure 6 Search results for 10 iterations

ISSN 2616-5767 Vol.8, Issue 4: 110-120, DOI: 10.25236/AJETS.2025.080415

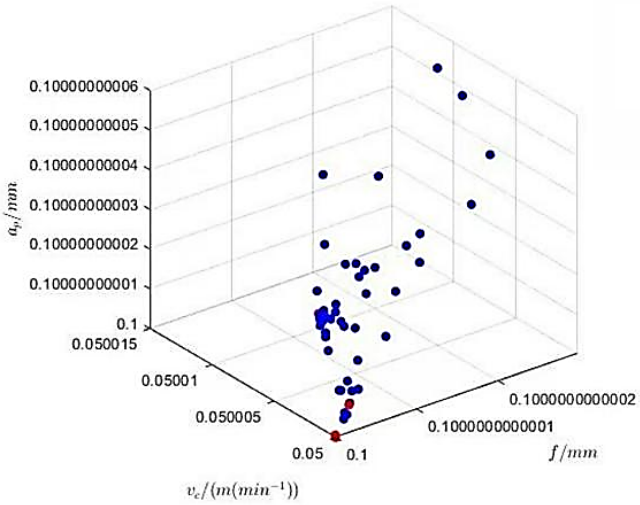

Figure 7 Search results for 50 iterations

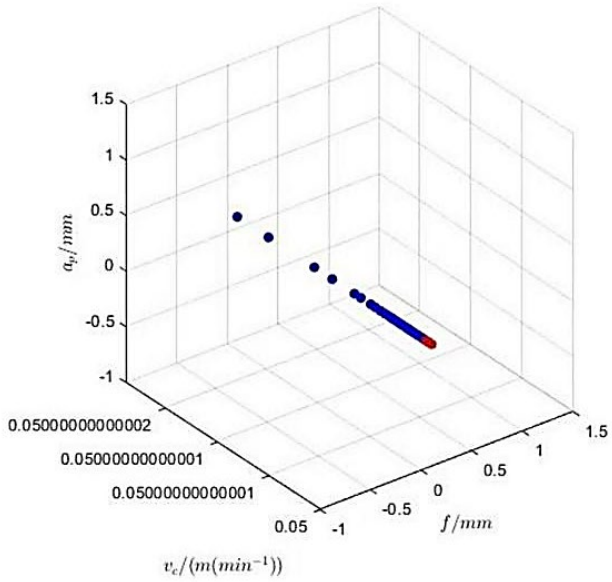

Figure 8 Search results for 100 iterations

Appropriate feed speed and back cutting amount is selected beneficial for processing time. From the overall optimization results(From figure 6 to figure 8), as the weight coefficient c increases, cutting time first decreases and then increases, and processing deformation also first decreases and then increases, which means that processing time is closely related to processing deformation, and there exists an optimal combination between the two.

5. Conclusion

An optimization model for CNC lathes with minimal processing time and deformation is established, and a black hole-continuous ant colony algorithm is proposed to find the optimal turning parameter method. The optimization algorithm combines the continuous ant colony algorithm with the black hole algorithm to expand the search range of the algorithm and solve local optimal parameters while improving convergence accuracy. The cutting parameters optimized using the black hole-continuous ant colony algorithm significantly reduce processing time and deformation compared to those obtained using empirical parameters. Compared to the ACO_R algorithm and $NSGA-\mathrm{II}$ algorithm, the $BH-ACO_R$ algorithm not only has a larger optimization range but also improves the overall optimization effect. Therefore, the $BH-ACO_R$ algorithm can effectively balance the requirements of processing efficiency and quality, providing an effective solution for enterprises to optimize processing technology and select suitable parameter combinations.

ISSN 2616-5767 Vol.8, Issue 4: 110-120, DOI: 10.25236/AJETS.2025.080415

References

[1] DORIGO M, GAMBARDELLA L M. Ant colony system: a cooperative learning approach to the traveling salesman problem [J]. IEEE Transactions on Evolutionary Computation, 1997,1(1):53-66.
[2] JIN TT, WU S F, LI S, et al. Research on improved ant colony algorithm for lightweight of main girders[J]. Machine Design and Manufacturing Engineering, 2019, 48(1):9-13. (in Chinese).
[3] DAI Y T, ZHAO X R, LIU L Q. Parameter identification of ship longitudinal motions using continuous ant colony algorithm with period searching[J]. Journal of ShipMechanics, 2010,14(8):872-878. (in Chinese).
[4] CAO T K, LIU Y J, XU Y T. Cutting performance of tool with continuous lubrication at tool-chip interface[J]. International Journal of Precision Engineering and Manufacturing-Green Technology, 2020, 7(2):347-359.
[5] LAN Z Q, LIANG Q Y. Analysis and Control of Machining Deformation Factors of Aero- engine Blades [J]. Scientific and Technological Innovation, 2019(4).
[6] SONG DD, XUE F, WU D D, et al. Iso-parametric Path-planning Method of Twin-tool Milling for Turbine Blades [J]. The International Journal of Advanced Manufacturing Technology,2018, 98(9): 3179—3189.
[7] K UMAR R, BILGA P S, SINGH S. Multi objective optimization using different methods of assigning weights to energy consumption responses, surface roughness and material removal rate during rough turning operation[J]. Journal of Cleaner Production,2017,164:45-57.
[8] Wang Dong, Xi Xinfu, Ge Xiaoyi, Sun Yize. Optimization Design of Latch Needle Mechanism in Warp Knitting Machine Using Improved Ant Colony Algorithm[J]. Machinery Design & Manufacture. 2023, 11(6).
[9] LI T, KONG LL, ZHANG H C, et al. Recent research and development of typical cutting machine tool's energy consumption model[J]. Journal of MechanicalEngineering,2014,50(7):102-111.
[10] Chen Hongsong, Dong Dingqian, Huang Bing, Liao Yinghua, Xu Yun, Zhang Wenke, Zhang Jiawei. Optimization of Milling Process Parameters for Aviation Blades Based on Genetic Algorithm[J]. Tool Engineering, 2021, 55(09): 68-73.